Supplementary Materials

In-Plane Anisotropic Thermal Conductivity of Low-Symmetry $PdSe_2$

Lijie Chen[1], Weitao Zhang[1], Hanlin Zhang[1], Jiawang Chen[1], Chaoyang Tan[1], Shiqi Yin[1], Gang Li[1]， Yu Zhang[1], Penglai Gong[2], and Liang Li[1, 3, *)]

1. Information Materials and Intelligent Sensing Laboratory of Anhui Province, Institutes of Physical Science and Information Technology, Anhui University, Hefei 230601, P. R. China
2. Department of Physics, Southern University of Science and Technology, Shenzhen 518055, P. R. China
3. Key Laboratory of Structure and Functional Regulation of Hybrid Materials (Anhui University), Ministry of Education, Institutes of Physical Science and Information Technology, Anhui University, Hefei 230601, P. R. China

* E-mail: liangli@ahu.edu.cn

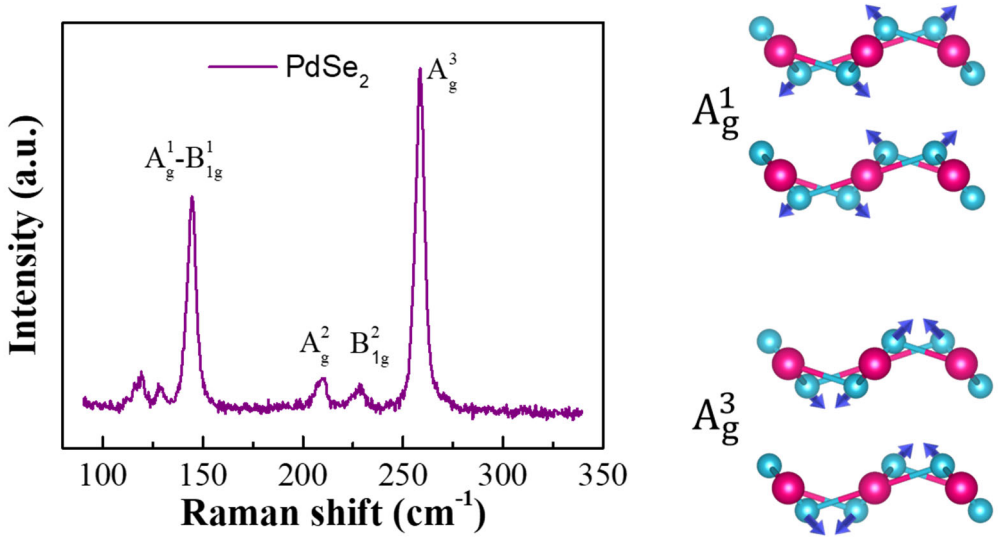

Figure S1. Typical Raman spectra of $PdSe_2$. The main peaks in the spectra for bulk structure and Raman-active vibrational modes of A_g^1 and A_g^3, Red: Pd atom, blue: Se atom.

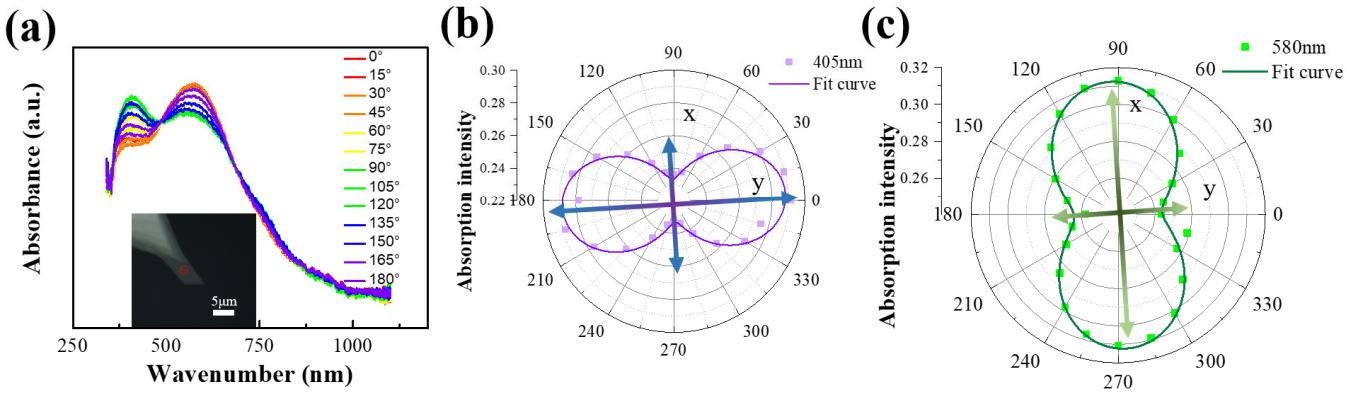

Figure S2. (a) Polarized light absorption spectrum shows the relationship between absorption intensity and polarization angle. (b) and (c) are polarization diagrams of light absorption at 405 and 580nm, respectively.

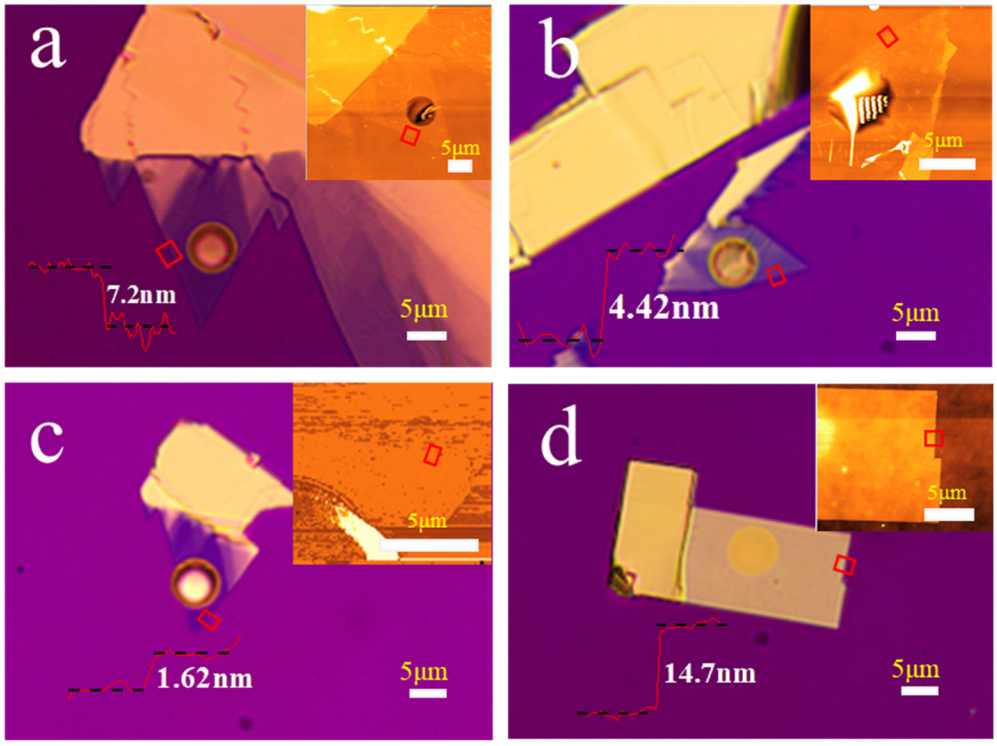

Figure S3. Optical imaging and AFM height profiles of suspended few-layered $PdSe_2$. The red rectangles represent the AFM measurement areas, and the red curves represent the height profile.

Note S1：Raman tensors fitting

To study the nature of vibrational anisotropy of $PdSe_2$, we employed the angle-resolved polarized Raman spectroscopy (ARPRS) spectrum. The variation rules of Raman intensity and deflection angle are studied systematically. The unit cell of $PdSe_2$ contains 12 atoms, and there are 36 phonon modes at the center of the Brillouin zone. The phonon vibration modes can be expressed as[1]

$$\Gamma = 3A_g + 3B_{1g} + 3B_{2g} + 3B_{3g} + 6A_u + 6B_{1u} + 6B_{2u} + 6B_{2u} + 6B_{3u} \quad (1)$$

Only A_g, B_{1g}, B_{2g}, and B_{3g} modes are Raman-active. The Raman intensity can be described by:

$$I \propto |e_i R e_s^T|^2 \quad (2)$$

R is the Raman tensor. The Raman tensor of the vibration mode of $PdSe_2$ can represent the following equation:

$$\mathrm{R(A_g)} = \begin{pmatrix} a & 0 & 0 \\ 0 & b & 0 \\ 0 & 0 & c \end{pmatrix}, \ \mathrm{R(B_{1g})} = \begin{pmatrix} 0 & d & 0 \\ d & 0 & 0 \\ 0 & 0 & 0 \end{pmatrix}$$
$$\mathrm{R(B_{2g})} = \begin{pmatrix} 0 & 0 & e \\ 0 & 0 & 0 \\ e & 0 & 0 \end{pmatrix}, \ \mathrm{R(B_{2g})} = \begin{pmatrix} 0 & 0 & 0 \\ 0 & 0 & f \\ 0 & f & 0 \end{pmatrix} \quad (3)$$

a~f represent the Raman tensors element, which is related to the space group structure of the unit cell. Where e_i and e_s represent the polarized unit vectors of the incident and scattered lights, respectively. The Raman intensity varies in parallel and cross configuration. In the experiment, the Raman signal is detected by backscatter mode. The e_i and e_s about parallel configuration can be defined as

$$e_i = (cos\theta, \ \ sin\theta, \ \ 0), \ e_j = (cos\theta, \ \ sin\theta, \ \ 0) \quad (4)$$

And cross configuration can be defined as

$$e_i = (cos\theta, \ \ sin\theta, \ \ 0), \ e_j = (-sin\theta, \ \ cos\theta, \ \ 0) \quad (5)$$

θ represents the angle between the orientation of the crystal and the polarization direction of the incident or scattered light. In the parallel configuration, the polarization of the incident light is parallel to the polarization of the scattered light, and in the cross configuration, the polarization of the incident light is perpendicular.

The relationship between the Raman strength of A_g and B_g and the deflection angle can be obtained by combining the above eqs (1) to (5).

$$I(A_g)^{\parallel} = (acos^2\theta + bsin^2\theta)^2 \quad (6)$$

$$I(A_g)^{\perp} = \left(\frac{b-a}{2} sin2\theta\right)^2 \quad (7)$$

$$I(B_{1g})^{\parallel} = (dsin2\theta)^2 \quad (8)$$

$$I(B_{1g})^{\perp} = (dsin2\theta)^2 \quad (9)$$

where $\parallel$ or $\perp$ demonstrate the parallel or perpendicular polarization.

Note S2: Determination of the average temperature profile through the boundary conditions

In our experiment, the heat dissipation equation in the suspended area and outside the hole can be described as [2, 3]:

$$\boldsymbol{\kappa \frac{1}{r}\frac{d}{dr}\left[r\frac{dT(r)}{dr}\right] + q(r) = 0\ (r < R)} \tag{10}$$

$$\boldsymbol{\kappa' \frac{1}{r}\frac{d}{dr}\left[r\frac{dT'(r)}{dr}\right] - \frac{G}{h}[T(r) - T_0] = 0\ (r > R)}, \tag{11}$$

$T(r)$ and $T'(r)$ are temperature distribution inside and outside the hole, respectively. T_0 is the room temperature (300 K). G is the interfacial thermal conductance between $PdSe_2$ and the substrate, its typical value is 50 MW $m^{-2}K^{-1}$ for van der Waals materials. Although this is a simplified spherical distribution equation, we are more concerned with the relationship between the thermal conductivity κ and the heat input. It is still applicable when applied in different directions. The volumetric optical heating q(r) is expressed as

$$q(r) = \frac{Ia}{h}\exp\left(-\frac{r^2}{r_0^2}\right) \tag{12}$$

where I is the peak absorbed laser power per unit area, α is the optical absorption of 532 nm obtained from the previous report [4], h is the thickness of the few-layer $PdSe_2$, and r_0 is the half of the Gaussian beam width of 1 μm.

By solving the heat dissipation equations in the main text, we can get the temperature profiles for both inside $T(r)$ and outside $T'(r)$ hole:

$$\boldsymbol{T(r) = c_1 - 2c_2 lnr + c_2 Ei\left[1, \left(\frac{r}{r_0}\right)^2\right]}, \tag{13}$$

$$\boldsymbol{T'(r) = c_3 K_0\left[0, r\sqrt{\frac{G}{\kappa' h}}\right] + T_0} \tag{14}$$

where K_0 is the Bessel function of the second kind, Ei is the exponential integral, and r_0 is the half of the Gaussian beam width of 1 μm in our Raman system. Based on the hole structure in our experiment, taking the boundary conditions into consideration:

$$\boldsymbol{T(R) = T'(R)} \tag{15}$$

$$\boldsymbol{T'(r) = T_0}\ \ (r \to \infty) \tag{16}$$

Therefore, the average temperature Tm inside the laser spot can be easily calculated by above equations.

We also evaluate the radiation heat loss for the suspended samples. The formula of radiation heat loss is expressed as $Qr = \varepsilon\sigma A(T^4 - T_0^4)$, where ε, σ and A respectively denote the emissivity, Stefan-Boltzmann constant and suspended graphene area, and T and T_0 are the temperatures of $PdSe_2$ and the environment, respectively. For example, in the thickness of 7.2 nm sample, taking ε = 1, T_0 = 300 K and T = 600 K, which high than ~ 500 μW incident laser

power based on the experimental results, Qr is calculated to be 0.193 μW for a 6 μm diameter suspended sample. The value of radiation heat loss is far less than the absorbed laser power 76 μW. Therefore, the radiation heat loss is negligible for all the measured samples.

NoteS3: The error bar of thermal conductance

The error bar of interfacial thermal conductance is obtained by propagating error from the uncertainty of the measured slope of the power and temperature. And then we extract the thermal conductivity κ. From the heat diffusion equation, the uncertainty of κ can be calculated from eq. 17 to eq. 19.

$$\frac{\boldsymbol{\delta\kappa}}{|\boldsymbol{\kappa}|} = \sqrt{\left(\frac{\boldsymbol{\delta T_m}}{|\boldsymbol{T_m}|}\right)^2 + \left(\frac{\boldsymbol{\delta P}}{|\boldsymbol{P}|}\right)^2} \tag{17}$$

$$\frac{\boldsymbol{\delta T_m}}{|\boldsymbol{T_m}|} = \frac{\boldsymbol{\delta \chi_T}}{|\boldsymbol{\chi_T}|} \tag{18}$$

$$\frac{\delta P}{|P|} = \frac{\delta \chi_p}{|\chi_p|} \tag{19}$$

For $PdSe_2$ suspended on Si_3N_4, we find that the fitting slopes along x-direction of frequency to temperature and excitation power function are χ_T = -0.00881±0.00123 cm^{-1}/K and χ_P = -0.00301±0.000358 cm^{-1}/mW, respectively. $\frac{\boldsymbol{\delta \chi_T}}{|\boldsymbol{\chi_T}|}$ = 0.1396 and $\frac{\boldsymbol{\delta \chi_p}}{|\boldsymbol{\chi_p}|}$ = 0.1189 was obtained, Finally. The result of $\frac{\boldsymbol{\delta\kappa}}{|\boldsymbol{\kappa}|}$ = 0.1834, $\kappa = \kappa \times 18.34\% = 25.35 \times 18.34\% = 4.648 Wm^{-1}K^{-1}$.

The fitting slopes along y-direction of frequency to temperature and excitation power function are χ_T = -0.00867 ± 0.000878 cm^{-1}/K and χ_P = -0.00264 ± 0.000129 cm^{-1}/mW, respectively. $\frac{\boldsymbol{\delta \chi_T}}{|\boldsymbol{\chi_T}|}$ = 0.1012 and $\frac{\boldsymbol{\delta \chi_p}}{|\boldsymbol{\chi_p}|}$ = 0.0489 was obtained, Finally. The result of $\frac{\boldsymbol{\delta\kappa}}{|\boldsymbol{\kappa}|}$ = 0.1124, $\delta\kappa = \kappa \times 11.24\% = 28.45 \times 18.34\% = 3.1978\ W\ m^{-1}K^{-1}$. The same analysis is also applied for other thickness and the calculation results are shown in the following Figure 4(c).

References

1. Yu, J.; Kuang, X.; Gao, Y.; Wang, Y.; Chen, K.; Ding, Z.; Liu, J.; Cong, C.; He, J.; Liu, Z.; Liu, Y., Direct Observation of the Linear Dichroism Transition in Two-Dimensional Palladium Diselenide. *Nano Lett.* **2020,** 20,1172-1182.
2. Peimyoo, N.; Shang, J.; Yang, W.; Wang, Y.; Cong, C.; Yu, T., Thermal conductivity determination of suspended mono- and bilayer WS_2 by Raman spectroscopy. *Nano Res.* **2014,** 8,1210-1221.
3. Chen, Y.; Peng, B.; Cong, C.; Shang, J.; Wu, L.; Yang, W.; Zhou, J.; Yu, P.; Zhang, H.; Wang, Y.; Zou, C.; Zhang, J.; Liu, S.; Xiong, Q.; Shao, H.; Liu, Z.; Zhang, H.; Huang, W.; Yu, T., In-Plane Anisotropic Thermal Conductivity of Few-Layered Transition Metal Dichalcogenide Td-WTe_2. *Adv. Mater.* **2019,** 31,1804979.
4. Oyedele, A. D.; Yang, S.; Liang, L.; Puretzky, A. A.; Wang, K.; Zhang, J.; Yu, P.; Pudasaini, P. R.; Ghosh, A. W.; Liu, Z.; Rouleau, C. M.; Sumpter, B. G.; Chisholm, M. F.; Zhou, W.; Rack, P. D.; Geohegan, D. B.; Xiao, K., $PdSe_2$: Pentagonal Two-Dimensional Layers with High Air Stability for Electronics. *J. Am. Chem. Soc.* **2017,** 139,14090-14097.